Effect of ^{6}Li resonances on near-barrier elastic scattering involving ^{28}Si and ^{58}Ni target nuclei

A. Gómez Camacho,[1] A. Diaz-Torres,[2] P. R. S. Gomes,[3] and J. Lubian[3]

[1]*Departamento de Aceleradores, Instituto Nacional de Investigaciones Nucleares, Apartado Postal 18-1027, C. P. 11801, Mexico, D. F.*

[2]*European Centre for Theoretical Studies in Nuclear Physics and Related Areas, Strada delle Tabarelle, 286, I-38123 Villazzano Trento, Italy*

[3]*Instituto de Fisica, Universidade Federal Fluminense, Avenida Litoranea s/n, Gragoatá, Niterói RJ 24210-340, Brazil*

(Received 5 September 2014; published 14 January 2015)

Calculations of elastic scattering angular distributions for reactions of the weakly bound projectile ^{6}Li with targets ^{28}Si and ^{58}Ni at energies just above the Coulomb barrier are performed with the continuum-discretized coupled-channel calculation method. Ground, resonant, and nonresonant continuum states of ^{6}Li are included in the convergent calculations. The effect of the resonances on elastic scattering angular distributions is studied, in an original procedure, by excluding from the continuum space those states corresponding to the resonances. When the resonances of ^{6}Li are considered, the calculated elastic scattering angular distributions are in good agreement with the measurements. The exclusion of the resonances, unexpectedly, has a very small effect at the energies studied. Calculation of the polarization potentials associated with the resonances show that they have a repulsive character at the long range region, where scattering occurs. It is also confirmed that couplings to continuum states of ^{6}Li are essential to achieve agreement with the data.

DOI: 10.1103/PhysRevC.91.014607 PACS number(s): 24.10.Eq, 24.30.−v, 25.60.Bx, 25.60.Gc

I. INTRODUCTION

In the last years, reaction mechanisms involving weakly bound nuclei, both stable and radioactive, have been a subject of strong research from experimental and theoretical viewpoints [1–3]. Since weakly bound nuclei can easily fragment into different components, the effects of breakup on elastic scattering and on fusion reaction mechanisms have been a central subject of study. Moreover, it is now known that couplings to continuum states of the weakly bound projectile have a strong effect not only on elastic scattering but on other reaction processes such as fusion. At energies close to the barrier, it has been found [4–8] that couplings to continuum states give rise to repulsive polarization potentials that decrease fusion absorption.

Among the most experimentally and theoretically studied weakly bound nuclei is ^{6}Li. Elastic, fusion, and breakup cross section measurements are available in a wide range of energies for the reaction of ^{6}Li with a large variety of target masses, such as ^{4}He, ^{12}C, ^{27}Al, ^{28}Si, ^{58}Ni, ^{59}Co, ^{144}Sm, and ^{208}Pb [9–19] . In the cluster model, the weakly bound stable nucleus ^{6}Li is portrayed with a α-d structure [10,20] with a ground state energy of -1.47 MeV and resonant states with $l = 2$, $j^{\pi} = 3^{+},2^{+}$, and 1^{+}. These states are identified to have energies $\varepsilon_{3+} = 0.71$, $\varepsilon_{2+} = 2.83$, $\varepsilon_{1+} = 4.18$ MeV (above threshold) and widths $\Gamma_{3+} = 0.024$, $\Gamma_{2+} = 1.7$, and $\Gamma_{1+} = 1.5$ MeV, respectively.

Since breakup processes involve unbound states of the projectile's fragments, an adequate theoretical tool to investigate the effect of breakup continuum states on elastic and fusion processes is the continuum-discretized coupled-channel model (CDCC) [12,21]. In this model, the continuum space is discretized in a finite number of states up to a maximum energy where the calculations converge. The purpose of the present work is to calculate the effect on elastic scattering angular distributions, of the resonant continuum states of the weakly bound nucleus $^{6}\mathrm{Li} \rightarrow d + \alpha$, in reactions with the ^{28}Si and ^{58}Ni targets, at energies around the Coulomb barrier. The usual CDCC calculations (see, for example, [4,12,16,20,22,23]) include these resonances in the whole continuum spectrum. In some works where CDCC calculations are not performed, as for example, those by Dasgupta *et al.* [24], the effect of breakup on the fusion cross section is approximately simulated by performing standard coupled channel calculations including the resonant states as excited bound states, in the case that the widths of the resonances are not so large and the resonances live a longer time than the reaction time.

In the present work we perform two kinds of calculations. The first is the usual one, with several energy bins, including the resonances. In the second, we exclude from the whole discretized energy states those around the resonances, in order to compare both results and have information concerning the role played by those resonances in the elastic scattering of ^{6}Li. In this way, we can disentangle the importance of couplings to resonance states in the CDCC calculations. On the same footing, the polarization potentials associated with couplings to resonance states are calculated and the effect of resonance couplings on elastic scattering may be explained in terms of these potentials.

The CDCC method is used with global d-target and α-target interactions which depend on the target mass A and incident collision energy E_{lab}. The global Woods-Saxon potentials of Ref. [25] are used for the d-target interaction V_{dT}. The parametrization of these potentials has been obtained by a large analysis of experimental elastic and inelastic cross sections for reactions of deuteron with a large variety of nuclear target masses ($12 < A < 238$) and range of incident energies ($E_{\mathrm{lab}} < 183$ MeV). This interaction is an improvement on other widely used systematic parametrizations [26–28]. The present calculations also test this improved parametrization of the V_{dT} interaction, when used to describe continuum states of the deuteron after the breakup of ^{6}Li in reaction with different targets. The density dependent double-folding Sao Paulo potential (SPP) [29], with adequate α-particle mass

densities, is used to describe the α-target interaction $V_{\alpha T}$. The SPP has been widely used with success to describe elastic and inelastic scattering, as well as nucleon transfer cross sections for a number of nuclear systems (see, for example [30–34]. An extensive systematics of nuclear densities has been performed in Ref. [30] to produce a parameter-free interaction. In our calculations, the α-target interaction depends only on the target mass A and kinetic energy of the α particle in respect to the initial incident energy of ^{6}Li. As for the α-d cluster structure of ^{6}Li, we use the Woods-Saxon parameterization given in Ref. [20]. Ground, unbound resonant, and nonresonant continuum scattering states of ^{6}Li are generated with this interaction.

The paper is organized as follows. In Sec. II, a brief description of the CDCC formalism is given. Section III addresses the CDCC calculations for elastic scattering angular distributions, polarization potentials, and how the effect of resonant continuum states of ^{6}Li is calculated. Finally, a summary is given in Sec. IV.

II. CDCC FORMALISM FOR A THREE-BODY SYSTEM

The ^{6}Li projectile is considered as a two-body nucleus, made of an α *particle* and a *deuteron*, which together with the target nucleus considered inert, form a three-body system. The ^{6}Li wave function reads as

$$\psi^P_{lsj}(\mathbf{r},k) = \left\{Y_{lm_l}(\hat{\mathbf{r}}) \otimes \chi_{I\mu s\sigma}\right\}_{lj} \frac{\varphi_l(r,k)}{r}, \tag{1}$$

where $\chi_{I\mu s\sigma}$ stands for the total internal wave function of both the α particle and deuteron (since the clusters are considered inert, $I = 0$, while $s = 1$ due to the deuteron spin); $\varphi_l(r,k)$ describes the α-d radial motion with asymptotic wave number k, orbital angular momentum l, and total angular momentum j. Equation (1) represents eigenstates of the projectile Hamiltonian, $\hat{h}_{\alpha d} = \hat{T}_{\mathbf{r}} + \hat{V}_{\alpha d}$, with eigenvalues ε_β, where $\beta \equiv \{lsjk\}$. $\beta = 0$ refers to the ^{6}Li ground state (g.s.). The remaining states are unbound (scattering and resonant) states. The continuum states $\varphi_l(r,k)$ in Eq. (1) are not square integrable, but the CDCC framework [12,21] provides a recipe for constructing square-integrable wave functions that are called *bin* states.

A bin state $u^{(i)}_\beta(r)$ is made of scattering wave functions within a given interval of continuum k values, $k_{i-1} < k < k_i$,

$$u^{(i)}_\beta(r) = \sqrt{\frac{2}{\pi\eta_l}} \int_{k_{i-1}}^{k_i} w_i(k,l) e^{-i\delta_k(l)} \varphi_{lsj}(r,k) dk, \tag{2}$$

where $\delta_k(l)$ are scattering phase shifts of φ_β. The weight functions $w_i(k,l)$ are usually unity, but for resonant bins $w_i(k,l) = \sin[\delta_k(l)]$, they satisfy,

$$\eta_l = \int_{k_{i-1}}^{k_i} |w_i(k,l)|^2 dk. \tag{3}$$

The energy $\varepsilon_\beta = \frac{\hbar^2}{2\mu_{\alpha d}}(k_{i-1} + k_i)^2/4$ is associated with the bin state of Eq. (2). These bin states along with the g.s. wave function are used as a discrete basis for expanding the total three-body wave function. That is, $\Psi(\mathbf{R},\mathbf{r}) = \sum_\beta F_\beta(\mathbf{R})\psi^P_\beta(\mathbf{r})\Phi^T_0$, where Φ^T_0 and $F_\beta(\mathbf{R})$ describe the inert target and the projectile-target relative motion in the β channel, respectively. This three-body wave function obeys the stationary Schrödinger equation with the asymptotic, Coulomb-wave boundary condition and the three-body Hamiltonian,

$$\hat{H} = \hat{T}_{\mathbf{R},\mathbf{K}} + \hat{h}_{\alpha d}(\mathbf{r},\mathbf{k}) + \hat{V}_{\alpha T}\left(\mathbf{R} + \tfrac{2}{6}\mathbf{r}\right) + \hat{V}_{dT}\left(\mathbf{R} - \tfrac{4}{6}\mathbf{r}\right), \tag{4}$$

where $\hat{T}_{\mathbf{R},\mathbf{K}}$ is the kinetic energy operator for the projectile-target relative motion, and $\hat{V}_{\alpha T}$ and $\hat{V}_{dT}$ denote the α particle and deuteron interactions with the target, respectively. Projecting this Schrödinger equation onto the $\psi^P_\beta(\mathbf{r})\Phi^T_0$ states, the following coupled equations are obtained,

$$\left[\hat{T}_R + U^{(J)}_{\beta\beta}(R) - E - \varepsilon_\beta\right] F^{(J)}_\beta(R) = -\sum_{\beta'} U^{(J)}_{\beta\beta'}(R) F^{(J)}_{\beta'}(R), \tag{5}$$

where $F^{(J)}_\beta(R)$ is the radial part of $F_\beta(\mathbf{R})$ with total angular momentum J. In Eq. (5), $U^{(J)}_{\beta\beta}(R)$ and $U^{(J)}_{\beta\beta'}(R)$ stand for radial dependent diagonal and nondiagonal matrix elements of the interaction potentials,

$$U^{(J)}_{\beta\beta'}(R) = \langle u_\beta | \hat{V}_{dT} + \hat{V}_{\alpha T} | u_{\beta'} \rangle, \tag{6}$$

where the integration is carried out over the target and projectile internal coordinates as well as the angular part of $\mathbf{R}$. The diagonal term $U^{(J)}_{00}(R)$ refers to the elastic optical potential; the couplings among the projectile states appear on the r.h.s in Eq. (5).

Details of the calculations

The CDCC calculations have been performed with the FRESCO code [35], using the following interaction potentials:

(i) The nuclear part of the deuteron-target potential V_{dT} is the global optical potential from Ref. [25]. Note that a parameterization for radii ($R_j = r_j A^{1/3}$) which differs from the FRESCO parametrization [$R_j = r_j(A_1^{1/3} + A^{1/3})$] has been used in Ref. [25], where $A_1 = 2$ and A refers to the target mass.

(ii) For the nuclear part of $V_{\alpha T}$, the Sao Paulo potential (SPP) has been used [29,30]. The SPP is a nonlocal, double-folding density-dependent and parameter-free potential. The bare interaction takes into account the Pauli nonlocality involving the exchange of nucleons between projectile and target. The bare nonlocal potential is connected with the local folding potential $V_F(r)$ through an effective energy dependence, as the following expression:

$$V_{\alpha T}(r, E_\alpha) = [N_R + iN_I] V_F(r) e^{-v^2_\alpha/c^2}, \tag{7}$$

where r is the separation between the α particle and target, v_α is their relative velocity, and c is the speed of light. The velocity dependence of the potential is essential to account for the data from sub-barrier to intermediate energies, about 200 MeV/nucleon. However, for the energy range of the present work, it is not important. The radial shape of the imaginary part has the same form as the real part, with normalization

TABLE I. Calculated and experimental values (MeV) for energies and widths of ^{6}Li resonances.

Res.	E_{cal}	Γ_{cal}	E_{exp}	Γ_{exp}
3^+	0.73	0.034	0.716	0.024
2^+	3.09	1.3	2.84	1.7
1^+	4.67	4.2	4.18	1.5

coefficients N_R and N_I. The values of $N_R = 1$ and $N_I = 0.78$ are widely used, since they were able to explain data for tens of systems [31]. The SPP, which has been widely used in tens of papers with the assumptions mentioned above, is, therefore, a parameter-free potential which depends only on the masses A_1, A_2 of the interacting nuclei and collision energy E_α. In our case, $A_1 = 4$, $A_2 = A_T$, and the collision energy is $E_\alpha = \frac{4}{6}E_{\rm lab}$.

(iii) Two potentials, $V_{\alpha d}$ (see Table I in Ref. [20]), have been used for generating the ^{6}Li g.s. and continuum states, respectively. A Woods-Saxon potential provides the correct g.s. (with an energy of $\varepsilon_0 = -1.47$ MeV and quantum numbers $n = 2, l = 0, j^\pi = 1^+$), while another Woods-Saxon potential including a spin-orbit term yields the $l = 2$ ($j^\pi = 3^+, 2^+, 1^+$) resonances whose features are in reasonable agreement with observations (see Table I), with the exception of the calculated 1^+ resonance width that is notably broader than the experimental value. However, we expect that this disagreement does not impact on the conclusions drawn in the present work, as the discretized breakup space (see below) has provided a good quantitative explanation of observed fusion excitation functions [20] as well as elastic-scattering differential cross sections [18] in low-energy collisions involving the ^{6}Li projectile.

The nuclear and Coulomb potential multipoles of both V_{dT} and $V_{\alpha T}$ up to the hexadecapole term ($Q \leqslant 4$) have been included in the calculations.

1. Breakup space for convergence

The discretization of the continuum is as follows. The maximum orbital angular momentum for the α-d relative motion is $l_{\max} = 3$; larger values do not have any effect on the calculations. So, bin states for $l = 0$ ($j^\pi = 1^+$) and $l = 1$ ($j^\pi = 0^-, 1^-, 2^-$) are constructed with step $\Delta\varepsilon = 0.5$ MeV up to $\varepsilon_{\max} = 6.8$ MeV. Finer and variable steps are used for resonant states $l = 2$ ($j^\pi = 3^+, 2^+, 1^+$).

For bin states $l = 3$ ($j^\pi = 4^+, 3^+, 2^+$) a larger step $\Delta\varepsilon = 1.0$ MeV is used. Convergence tests at $\varepsilon_{\max} = 7.0, 7.5$, and 8.0 MeV were done with no effect on elastic angular distributions. Similarly, larger steps $\Delta\varepsilon = 0.75$ and 1.0 MeV were used with no appreciable effect on elastic scattering.

2. Separating the effect of resonances on the elastic scattering

It is very difficult (if not impossible) to separate the resonant continuum from the nonresonant one completely, as the features of the scattering states as a function of the energy are determined by the $V_{\alpha d}$ potential. However, the continuum-discretization procedure facilitates such a separation as follows. A resonant bin state is constructed with Eq. (2) using scattering states within an energy window determined by the resonance width (see Table I); a single bin state or a group of bins are associated to the centroid energy of the resonance. The resonant bins with $l = 2$ ($j^\pi = 3^+, 2^+, 1^+$) can be either included or removed from the set of coupled equations (5), allowing us to study their role in the elastic-scattering differential cross section. Please note that there is still some ambiguity in the present separation procedure as scattering states lying at the tail of the resonance strength function may be included in the nonresonant continuum bins. Nevertheless, the present work sheds light on the effect of specific ^{6}Li resonant states on the elastic-scattering angular distribution.

III. RESULTS OF THE CDCC CALCULATIONS: EFFECT OF RESONANCES

In this section CDCC calculations of elastic scattering angular distributions are presented for the projectile ^{6}Li with targets ^{28}Si and ^{58}Ni, for incident energies just above the corresponding Coulomb barriers. Figure 1 shows the calculations (solid lines) for elastic scattering cross section for ^{6}Li with target ^{28}Si at several incident energies around the barrier, where the data are those reported in Refs. [36–39]. The calculations with all couplings have, in general, a good agreement with the data. In some cases the agreement is not as good, owing to the fact that global interactions are used for the fragment-target subsystems. The dashed lines in these figures represent the calculations with states corresponding to the resonances omitted from the complete discrete space (the so called "second kind of calculation"). In this calculation ground and nonresonant breakup states are the same as those used in the full calculation with all couplings. It can be observed that the results of elastic scattering without couplings to resonance states have a negligible effect. Only at the lower energies

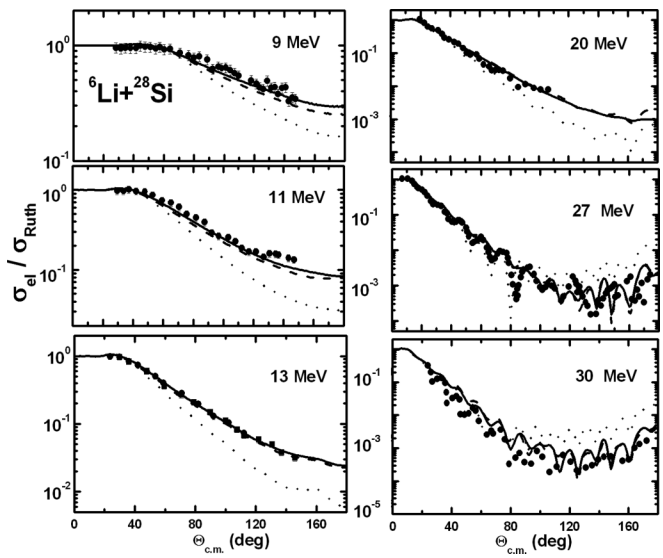

FIG. 1. Elastic scattering angular distributions for ^{6}Li + ^{28}Si. See text for details.

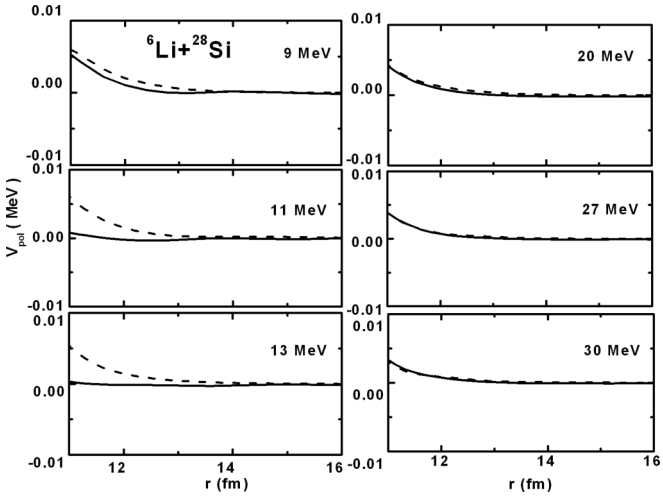

FIG. 2. Polarization potentials associated with couplings to the whole discrete space of ^{6}Li (solid lines) and without resonance space (dashed lines).

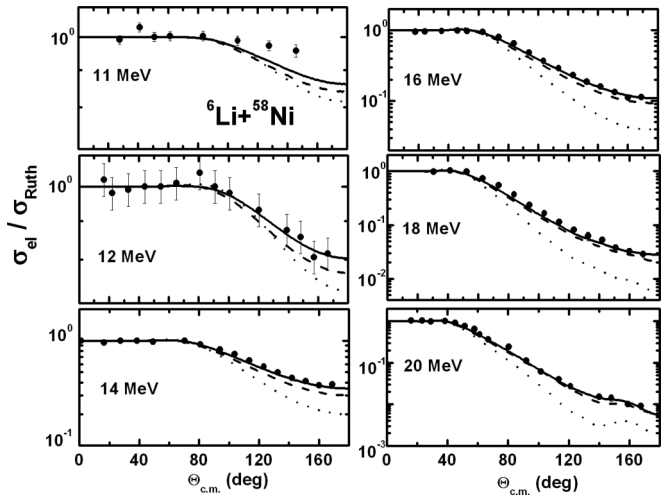

FIG. 4. Elastic scattering angular distributions for ^{6}Li + ^{58}Ni. See text for details.

some small effect may be observed, at backward angles. The calculations corresponding to the elastic channel coupling, that is, when only the term with $\beta = 0$ is considered in Eq. (5), with no couplings to continuum states, are represented by the dotted lines, which are not in agreement with the data. These results show that couplings to continuum states of ^{6}Li are essential to achieve agreement to the data.

To further investigate the effect of continuum resonance states of the projectile on elastic scattering, a calculation of the polarization potentials that emerge from couplings to these states has been performed. This has been done using the prescription given in Ref. [40]. The polarization potential ΔV is defined as the potential produced by couplings of the elastic scattering to other reaction channels, important at near barrier energies, leading to an effective potential $V_{\rm eff} = U_{00} + \Delta V$, where $U_{0,0}$ is the optical potential for the elastic channel given in Eq. (6). Figure 2 shows the results for the polarization potentials associated with the calculations when couplings between the whole discrete space of ^{6}Li (solid lines) are used. Also, the potentials without resonant state couplings are shown (dashed lines). As can be observed, these latter potentials present a less repulsive character with respect to the full calculation. So, the inclusion of couplings to resonant states provides a net repulsive polarization potential, and not an attractive polarization potential, as it is found when the resonant state is considered as a bound excited state. Indeed, this repulsive potential becomes less strong as the energy increases as shown in Fig. 3 for $E_{\rm lab} = 99$ MeV. Here, the top figure shows the calculation of elastic scattering angular distribution with the full spectrum (solid line) which is in reasonable agreement with the data [41]. The dashed and dotted lines represent the results without resonant continuum states and the elastic channel, respectively. The bottom

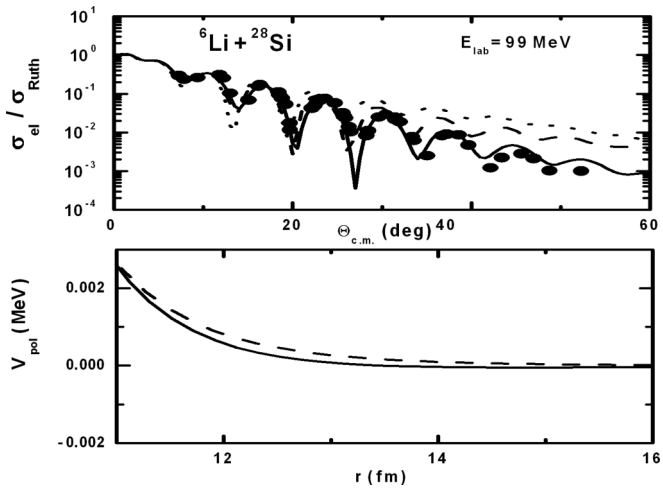

FIG. 3. Elastic scattering angular distribution calculation for ^{6}Li + ^{28}Si at $E_{\rm lab} = 99$ MeV and corresponding polarization potentials with and without resonances.

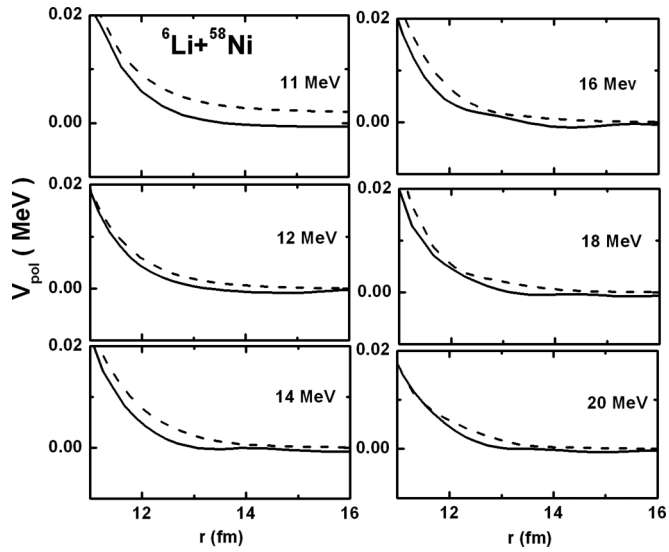

FIG. 5. Polarization potentials associated with couplings to the whole discrete space of ^{6}Li (solid lines) and without resonance space (dashed lines). See text for details.

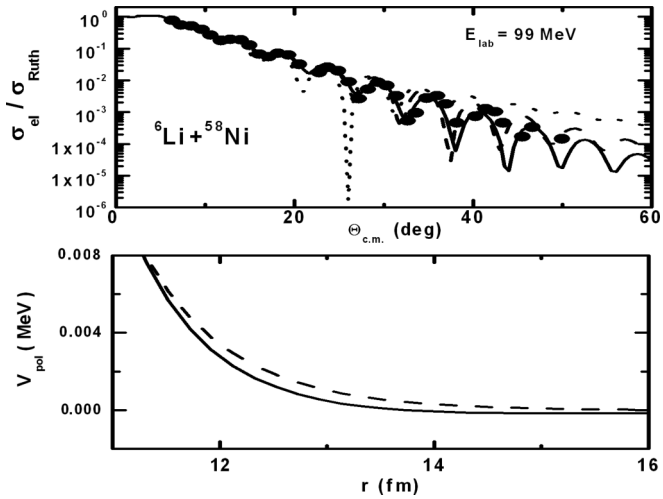

FIG. 6. Elastic scattering angular distribution calculation for ^{6}Li + ^{58}Ni at $E_{\rm lab} = 99$ MeV and corresponding polarization potentials with and without resonances.

figure shows a negligibly less repulsive polarization potential corresponding to the calculation without resonances (dashed line) respect to the full discrete spectrum calculation (solid line). Thus, as before, the inclusion of breakup resonant states of ^{6}Li provides a repulsive polarization potential. These results are in agreement with the well known fact that breakup reactions give rise to a repulsive polarization potential that is particularly strong at low bombarding energies.

Figure 4 shows the results for the ^{6}Li + ^{58}Ni reaction. As can be observed, elastic scattering cross section calculations (solid lines) are, in general, in good agreement with the data of Refs. [42,43]. The effect of omitting resonance couplings (dashed lines) are slightly observed at low energies while in all cases, coupling to only the elastic channel (dotted lines) is insufficient to fit the data. Figure 5 shows the results for the polarization potentials for the full space calculation (solid lines) and without resonances (dashed lines). Similar conclusions are obtained for this system as those mentioned above for ^{6}Li + ^{28}Si. Couplings to resonant continuum states of ^{6}Li become progressively less important as the energy increases as can be observed in Fig. 6 for ^{6}Li + ^{58}Ni at $E_{\rm lab} = 99$ MeV. The top figure shows elastic scattering calculations for the full discrete space (solid line) which is in good agreement with the data of Ref. [44]. The dashed line corresponds to the calculation without resonance states of ^{6}Li and the dotted line the single elastic channel one. The bottom figure of Fig. 6 shows the polarization potentials for the full spectrum (solid line) and without resonances (dashed line), where it is observed that the effect of omitting the resonances is even less important at higher than at lower energies.

IV. SUMMARY AND CONCLUSIONS

CDCC calculations of elastic scattering angular distributions have been performed for the nuclear systems ^{6}Li + ^{28}Si and ^{6}Li + ^{58}Ni at energies around the Coulomb barrier. In the calculations, the cluster structure of the projectile $^6\text{Li} \rightarrow \alpha + d$ is assumed and global interactions for the α-target and d-target subsystems are used. In general, good agreement between the calculations and the data has been achieved.

Using an original technique, the effect on elastic scattering due to couplings to resonance states of ^{6}Li, namely, $l = 2$, $J^\pi = 3^+, 2^+$, and 1^+ has been studied. This effect is calculated by extracting from the whole energy discrete space of ^{6}Li, the states corresponding to the resonances. That is, couplings to and between resonance states are not allowed. For both systems, only a very small effect is observed at the lowest energies. Thus, in most cases, couplings to resonance states are negligible. However, when couplings to the whole continuum spectrum are omitted, that is the calculation with only the elastic channel, the results are insufficient to fit the data. Therefore, couplings to the rest of the continuum spectrum of ^{6}Li are very important, although those to the resonance space *per se* are not.

The effect of resonance states is better understood in terms of the polarization potentials produced by couplings to these states. So, calculations of polarization potentials for the full discrete energy space and also without resonance states have been performed. A comparison of these potentials show that when the resonance states are omitted, a less repulsive potential emerges, respect to the full energy space. This result shows that resonance states produce a net repulsive potential. This conclusion is not surprising since it is well known that for many weakly bound nuclei, breakup states give rise to virtual repulsive polarization potentials that increase the fusion barrier (Coulomb + bare potentials) and consequently lower fusion absorption.

In summary, the results of our studies show that for the present systems at energies around the Coulomb barrier, the effect of breakup through resonant states on the elastic scattering is almost negligible. It would be interesting to study this effect on the elastic scattering angular distributions for heavier nuclei.

ACKNOWLEDGMENTS

Fruitful and interesting discussions are acknowledged with participants of the Workshop *Low-Energy Reaction Dynamics of Heavy-Ions and Exotic Nuclei* held at ECT*, Trento, May 26–30, 2014. Financial support received: A.G.C. from CONACYT, México; P.R.S.G. and J.L. from CNPq, FAPERJ, Pronex, Brazil.

[1] L. F. Canto, P. R. S. Gomes, R. Donangelo, and M. S. Hussein, Phys. Rep. **424**, 1 (2006).
[2] J. F. Liang and C. Signorini, Int. J. Mod. Phys. E **14**, 1121 (2005).
[3] N. Keeley, R. Raabe, N. Alamanos, and J. L. Sida, Prog. Part. Nucl. Sci. **59**, 579 (2007).
[4] S. Santra, S. Kailas, K. Ramachandran, V. V. Parkar, V. Jha, B. J. Roy, and P. Shukla, Phys. Rev. C **83**, 034616 (2011).

[5] L. F. Canto, J. Lubian, P. R. S. Gomes, and M. S. Hussein, Phys. Rev. C **80**, 047601 (2009).
[6] J. Lubian, T. Correa, P. R. S. Gomes, and L. F. Canto, Phys. Rev. C **78**, 064615 (2008).
[7] J. Lubian, T. Correa, E. F. Aguilera, L. F. Canto, A. Gomez-Camacho, E. M. Quiroz, and P. R. S. Gomes, Phys. Rev. C **79**, 064605 (2009).
[8] D. S. Monteiro *et al.*, Phys. Rev. C **79**, 014601 (2009).
[9] K. Rusek, P. V. Green, P. L. Kerr, and K. W. Kemper, Phys. Rev. C **56**, 1895 (1997).
[10] C. Beck, N. Keeley, and A. Diaz-Torres, Phys. Rev. C **75**, 054605 (2007).
[11] J. P. Fernandez-Garcia *et al.*, Phys. Lett. B **693**, 310 (2010).
[12] Y. Sakuragi, M. Yahiro, and M. Kamimura, Prog. Theor. Phys. Suppl. **89**, 1 (1986).
[13] K. Zerva *et al.*, Phys. Rev. C **80**, 017601 (2009).
[14] K. Rusek, N. Keeley, A. Pakou, and N. Alamanos, Nucl. Phys. A **784**, 13 (2007).
[15] A. Pakou *et al.*, Phys. Lett. B **633**, 691 (2006).
[16] N. Keeley, R. S. Mackintosh, and C. Beck, Nucl. Phys. A **380**, 1 (2010).
[17] N. Keeley and K. Rusek, Phys. Lett. B **375**, 9 (1996).
[18] D. R. Otomar, J. Lubian, and P. R. S. Gomes, Eur. Phys. J. A **46**, 285 (2010).
[19] G. R. Kelly *et al.*, Phys. Rev. C **63**, 024601 (2000).
[20] A. Díaz-Torres, I. J. Thompson, and C. Beck, Phys. Rev. C **68**, 044607 (2003).
[21] N. Austern, Y. Iseri, M. Kamimura, M. Kawai, G. Rawitscher, and M. Yahiro, Phys. Rep. **154**, 125 (1987).
[22] Y. Sakuragi, M. Yahiro, and M. Kimimura, Prog. Theor. Phys. **68**, 322 (1982).
[23] A. Shrivastava *et al.*, Phys. Lett. B **633**, 463 (2006).
[24] M. Dasgupta *et al.*, Phys. Rev. Lett. **82**, 1395 (1999); Phys. Rev. C **66**, 041602(R) (2002); **70**, 024606 (2004).
[25] H. An and C. Cai, Phys. Rev. C **73**, 054605 (2006).
[26] C. M. Perey and F. G. Perey, At. Data Nucl. Data Tables **13**, 293 (1974).
[27] W. W. Daehnick, J. D. Childs, and Z. Vrcelj, Phys. Rev. C **21**, 2253 (1980).
[28] J. Bojowald, H. Machner, H. Nann, W. Oelert, M. Rogge, and P. Turek, Phys. Rev. C **38**, 1153 (1988).
[29] L. C. Chamon, D. Pereira, M. S. Hussein, M. A. Cándido Ribeiro, and D. Galetti, Phys. Rev. Lett. **79**, 5218 (1997).
[30] L. C. Chamon *et al.*, Phys. Rev. C **66**, 014610 (2002).
[31] M. A. G. Alvarez *et al.*, Nucl. Phys. A **723**, 93 (2003).
[32] L. R. Gasques, L. C. Chamon, P. R. S. Gomes, and J. Lubian, Nucl. Phys. A **764**, 135 (2006).
[33] E. Crema, L. C. Chamon, and P. R. S. Gomes, Phys. Rev. C **72**, 034610 (2005).
[34] J. J. S. Alves *et al.*, Nucl. Phys. A **748**, 59 (2005).
[35] I. J. Thompson, Comput. Phys. Rep. **7**, 167 (1988).
[36] A. Pakou *et al.*, Phys. Lett. B **556**, 21 (2003).
[37] J. E. Poling, E. Norbeck, and R. R. Carlson, Phys. Rev. C **13**, 648 (1976).
[38] J. Cook, Nucl. Phys. A **375**, 238 (1982).
[39] M. F. Vineyard, J. Cook, and K. W. Kemper, Nucl. Phys. A **405**, 429 (1983).
[40] I. J. Thompson *et al.*, Nucl. Phys. A **505**, 84 (1989).
[41] P. Schwandt *et al.*, IUCF Annual Report, 1979, p. 82.
[42] E. F. Aguilera *et al.*, Phys. Rev. C **79**, 021601(R) (2009).
[43] K. O. Pfeiffer, E. Speth, and K. Bethge, Nucl. Phys. A **206**, 545 (1973).
[44] P. Schwandt *et al.*, IUCF Annual Report, 1980, p. 126.